Accurate mode characterization of two-mode optical fibers by in-fiber acousto-optics

E. Alcusa-Sáez, A. Díez,* and M. V. Andrés

Departamento de Física Aplicada y Electromagnetismo-ICMUV, Universidad de Valencia, Dr. Moliner 50, E-46100 Spain

*antonio.diez@uv.es

Abstract: Acousto-optic interaction in optical fibers is exploited for the accurate and broadband characterization of two-mode optical fibers. Coupling between LP_{01} and LP_{1m} modes is produced in a broadband wavelength range. Difference in effective indices, group indices, and chromatic dispersions between the guided modes, are obtained from experimental measurements. Additionally, we show that the technique is suitable to investigate the fine modes structure of LP modes, and some other intriguing features related with modes' cut-off.

OCIS codes: (060.2270) Fiber characterization; (230.1040) Acousto-optical devices.

References and links

1. D. Östling and H. E. Engan, "Narrow-band acousto-optic tunable filtering in a two-mode fiber," Opt. Lett. **20**(11), 1247–1249 (1995).
2. H. S. Kim, S. H. Yun, I. K. Kwang, and B. Y. Kim, "All-fiber acousto-optic tunable notch filter with electronically controllable spectral profile," Opt. Lett. **22**(19), 1476–1478 (1997).
3. T. A. Birks, P. S. Russell, and D. O. Culverhouse, "The acousto-optic effect in single-mode fiber tapers and couplers," J. Lightwave Technol. **14**(11), 2519–2529 (1996).
4. A. Díez, T. A. Birks, W. H. Reeves, B. J. Mangan, and P. St. J. Russell, "Excitation of cladding modes in photonic crystal fibers by flexural acoustic waves," Opt. Lett. **25**(20), 1499–1501 (2000).
5. M. W. Haakestad and H. E. Engan, "Acoustooptic properties of a weakly multimode solid core photonic crystal fiber," J. Lightwave Technol. **24**(2), 838–845 (2006).
6. E. P. Alcusa-Sáez, A. Díez, M. González-Herráez, and M. V. Andrés, "Improved time-resolved acousto-optic technique for optical fiber analysis of axial non-uniformities by using edge interrogation," Opt. Express **23**(6), 7345–7350 (2015).
7. E. P. Alcusa-Sáez, A. Díez, and M. V. Andrés, "Experimental analysis of distributed pump absorption and refractive index changes in Yb-doped fibers using acousto-optic interaction," Opt. Lett. **40**(5), 689–692 (2015).
8. S. Randel, R. Ryf, A. Sierra, P. J. Winzer, A. H. Gnauck, C. A. Bolle, R. J. Essiambre, D. W. Peckham, A. McCurdy, and R. Lingle, Jr., "6×56-Gb/s mode-division multiplexed transmission over 33-km few-mode fiber enabled by 6×6 MIMO equalization," Opt. Express **19**(17), 16697–16707 (2011).
9. J. W. Nicholson, A. D. Yablon, S. Ramachandran, and S. Ghalmi, "Spatially and spectrally resolved imaging of modal content in large-mode-area fibers," Opt. Express **16**(10), 7233–7243 (2008).
10. P. Hamel, Y. Jaouën, R. Gabet, and S. Ramachandran, "Optical low-coherence reflectometry for complete chromatic dispersion characterization of few-mode fibers," Opt. Lett. **32**(9), 1029–1031 (2007).
11. W. V. Sorin, B. Y. Kim, and H. J. Shaw, "Phase-velocity measurements using prism output coupling for single- and few-mode optical fibers," Opt. Lett. **11**(2), 106–108 (1986).
12. J. M. Savolainen, L. Grüner-Nielsen, P. Kristensen, and P. Balling, "Measurement of effective refractive-index differences in a few-mode fiber by axial fiber stretching," Opt. Express **20**(17), 18646–18651 (2012).
13. C. Tsao, *Optical Fibre Waveguide Analysis* (Oxford, 1992).
14. H. E. Engan, B. Y. Kim, J. N. Blake, and H. J. Shaw, "Propagation and optical interaction of guided acoustic waves in two-mode optical fibers," J. Lightwave Technol. **6**(3), 428–436 (1988).
15. D. L. Franzen, "Determining the effective cutoff wavelength of single-mode fibers: an lnterlaboratory Comparison," J. Lightwave Technol. **3**(1), 128–134 (1985).

1. Introduction

Acousto-optic (AO) interaction in optical fibers, whose operation principles are known since the 90s, has been exploited over the years for the development of dynamic and reconfigurable all-fiber devices. In the literature, one can find filters, equalizers, frequency shifters and

#255185 Received 4 Dec 2015; revised 22 Jan 2016; accepted 27 Jan 2016; published 26 Feb 2016

switches based on the interaction between an acoustic mode –either flexural, longitudinal or torsional mode–, and optical modes propagating in the fiber [1–3].

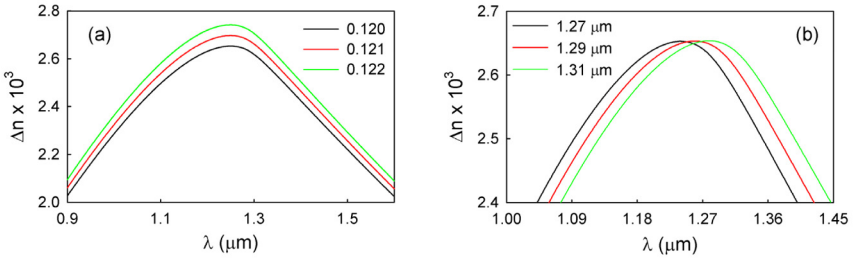

Fig. 1. Theoretical calculation of the LP_{01}-LP_{11} modal effective index difference, Δn, for different step-index silica optical fibers. (a) Fibers with 1.28 μm cutoff wavelength, and different NA (indicated in the figure), and (b) fibers with NA = 0.12, and different cutoff wavelengths (indicated in the figure). In all cases, the cladding diameter was 125 μm.

AO coupling has also been exploited as a technique to investigate the properties of optical fibers [4, 5]. Recently, time-resolved in-fiber acousto-optics was utilized for the characterization of axial diameter variations –in the order of nm– along an optical fiber [6], and to analyze refractive index changes produced by an optical pump in doped fibers [7].

With the advent of new strategies to develop optical transmission systems with larger capacity based on space-division multiplexing (SDM), few-mode fibers have gained relevancy again. A two-mode optical fiber provides six spatial channels in a single fiber [8]. Accurate characterization of the propagation properties of the different fiber modes is essential for the design of SDM schemes. Several methods for the characterization of few-mode fibers have been proposed. Most of them give information about the difference in group index or chromatic dispersion between the guided modes [9, 10]. Very few methods for measuring difference in modal effective (phase) indices have been reported so far [11, 12]. Differences in modal effective index is a key property for few-mode fiber systems because it governs the intermodal coupling. In this work, we explore the use of AO in optical fibers as a non-interferometric technique for a complete characterization of two-mode optical fibers.

2. Basis

An acoustic wave that propagates along an optical fiber creates a travelling periodic refractive-index perturbation that can cause coupling between co-propagating modes. When the acoustic wave is a flexural mode, the coupling occurs between modes with symmetric and antisymmetric field distribution across the fiber: coupling between the fundamental LP_{01} mode and modes of the series LP_{1m} (m = 1, 2,...) is enabled. Maximum coupling between two modes is achieved at the optical wavelength at which the phase-matching condition is satisfied, i.e., when the acoustic wavelength matches the beatlength between the two optical modes. The resonance wavelength, λ_R, is given by,

$$\lambda_R = \Delta n \cdot \Lambda \qquad (1)$$

where Λ is the acoustic wavelength, and Δn is the difference in effective index between the two optical modes. Equation (1) indicates that Δn can be obtained at the resonance wavelength by measuring λ_R, provided that the acoustic wavelength is known. The dependence of Δn with the optical wavelength, λ, can be determined by measuring λ_R for different values of Λ.

Figure 1 shows the LP_{01}-LP_{11} modal index difference as a function of wavelength, calculated for a silica optical fiber with 125 μm cladding diameter, and different values of NA and cut-off wavelength (λ_c). We assumed here a simple, step-index fiber geometry surrounded by air. The exact modes for such a three-layer fiber have been detailed in [13]. In all cases, Δn

#255185 Received 4 Dec 2015; revised 22 Jan 2016; accepted 27 Jan 2016; published 26 Feb 2016

shows a maximum centred close to the cut-off wavelength. Obviously, for wavelengths below cut-off the LP_{11} mode is guided by the core, while it has evolved to a cladding mode for wavelengths above cut-off. The two guiding regimes for the LP_{11} mode are at the origin of the different slope sign of Δn at both sides of the maximum. It can remarked that the two characteristic parameters of the fiber, i.e. NA and λ_c, produce changes in the curve Δn(λ) in different ways, at least within a given range. While a change of NA introduces a vertical shift, increasing Δn for all wavelengths, a change of λ_c shifts the wavelength at which Δn is maximum. It is worth to note that a small change of NA leads to a remarkable increase of Δn. Therefore, NA and λ_c of a two-mode optical fiber can be determined accurately and without ambiguity from measurements of Δn performed in a broadband wavelength range around the LP_{11} cutoff wavelength.

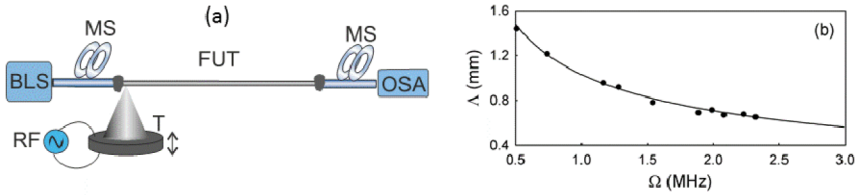

Fig. 2. (a) Experimental arrangement: BLS: broadband light source; MS: mode stripper; FUT: fiber under test; T: piezoelectric transducer. (b) Wavelength of the flexural elastic wave on the fiber as a function of its frequency. Dots are experimental measurements. Solid line is the theoretical calculation for the fundamental flexural elastic mode propagating in a 125 μm diameter silica optical fiber

On the other hand, if the dependence of Δn with the optical wavelength is known with accuracy, it is then a simple matter to obtain numerical derivatives of Δn with respect to wavelength. Hence, the group index difference, Δn_g, and the chromatic dispersion difference, ΔD, of the fiber modes can be investigated since,

$$\Delta n_g = \Delta n - \lambda \cdot \frac{d}{d\lambda}\Delta n \;; \quad \Delta D = -\frac{\lambda}{c} \cdot \frac{d^2}{d\lambda^2}\Delta n \tag{2}$$

where *c* is the speed of light in vacuum.

3. Experimental results and discussion

3.1 Experimental arrangement

Figure 2 shows a diagram of the experimental setup. Flexural elastic waves were generated by a piezoelectric transducer (provided by Morgan Advanced Ceramic), and were launched along an uncoated section of the fiber under test via an aluminium horn. The piezoelectric transducer was able to operate up to 10 MHz, and it was driven by an RF signal generator. The fiber was illuminated using an unpolarized broadband light source. The spectrum of the light transmitted through the fiber was recorded with an OSA. At the input of the fiber section, a mode stripper was inserted to ensure that only light carried by the LP_{01} mode enters the interaction region. A second mode stripper was inserted at the end of the interaction region to remove the light carried by the LP_{11} mode that was transferred from the input LP_{01} mode by the elastic wave. In this way, coupling between the two modes leads to a notch in the spectrum of the light that remains guided by the core. The notch can be tuned by changing the wavelength of the acoustic wave, Λ, which can be done by simply changing the frequency of the RF signal generator, Ω. The relationship between the frequency Ω and wavelength of the elastic wave Λ is determined by the dispersion relation of the flexural mode. In a first experiment, we investigated the dispersion properties of the elastic waves propagating along the fiber. Experimental measurements were performed using an optical vibrometer. We also calculated theoretically the dispersion of the fundamental flexural elastic mode propagating in

#255185 Received 4 Dec 2015; revised 22 Jan 2016; accepted 27 Jan 2016; published 26 Feb 2016

a silica optical fiber following the methods described in [14]. Both results are shown in Fig. 2(b), with good agreement between theory and experimental data.

3.2 Modal effective index difference

We investigated the properties of two commercially available optical fibers: Corning SMF-28e and SM2000 (commercialized by Thorlabs). The nominal values of the fiber characteristic parameters are included in Table 1. Figures 3(a)-3(b) show the resonance wavelength as a function of frequency for different couplings between the fundamental LP_{01} mode and LP_{1m} modes.

Notice that all the LP_{1m} modes, except the LP_{11} mode for wavelengths below its cutoff, are cladding modes within the wavelength range of the experiment. For a given frequency, the lower is the order of the LP_{1m} mode, the shorter is the resonance wavelength. When coupling to cladding modes, the resonance wavelength decreases as the frequency of the elastic wave increases, as expected [2]. However, the trend is more complex for the LP_{01}-LP_{11} coupling as a result of the two guiding regimes of the LP_{11} mode, which depends on the optical wavelength. For some frequencies, a particular feature is observed experimentally: the LP_{01}-LP_{11} coupling gives rise to two notches in the spectrum. This happens because phase-matching is satisfied simultaneously at two different wavelengths.

Table 1. Nominal characteristics of the fibers and best-fit parameters

	Nominal values		***Best-fit values***	
Fiber	λ_c	***NA***	λ_c	***NA***
SMF-28e	1.27 μm	0.14	1.40 μm	0.121
SM2000	1.7 μm	0.11	1.67 μm	0.119

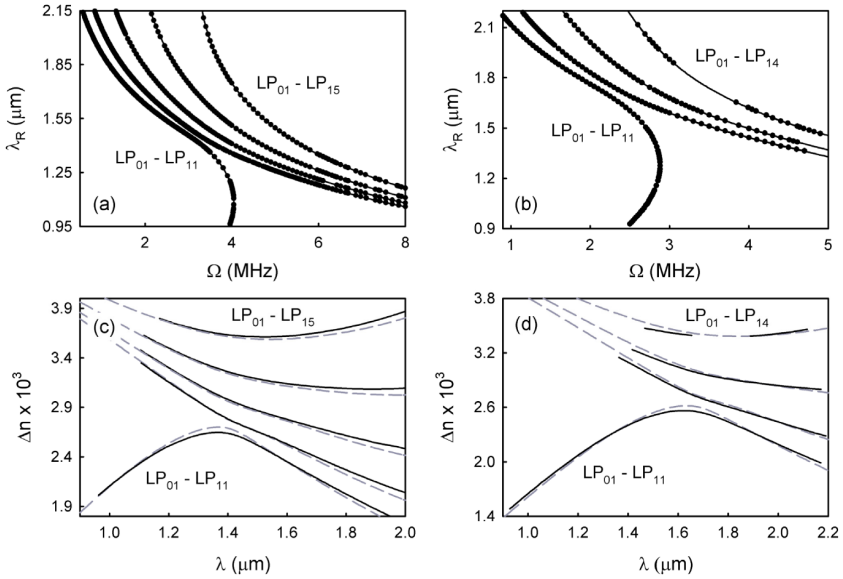

Fig. 3. (top) Resonance wavelength vs. frequency of the elastic wave, for different resonances. Dots are experimental data and solid line is a guide to the eye. (bottom) Modal indices difference vs. wavelength. Solid lines show the results obtained from the experiment. Dashed lines are theoretical calculations assuming a step-index profile. FUT: (a), (c) SMF-28e; (b), (d) SM2000.

Using Eq. (1) and the dispersion relation of the flexural elastic mode, the modal phase index difference was obtained as a function of wavelength from the experimental data shown in Figs. 3(a)-3(b). The results are shown in Figs. 3(c)-3(d). Additionally, theoretical calculations of Δn were performed for a 125μm fiber with a step refractive index profile. By

#255185 Received 4 Dec 2015; revised 22 Jan 2016; accepted 27 Jan 2016; published 26 Feb 2016

varying NA and λ_c in the model, numerical calculations were fitted to experimental data. The numerical results that best fit the experimental data are included in Figs. 3(c)-3(d). Table 1 gives the resulting best-fit parameters. In general terms, the step-index model describes properly the experimental results of Δn. The fiber parameters provided by the model for the SM2000 fiber are in good agreement with the nominal data provided by the manufacturer. However, for the SMF-28e the agreement in not so good, the NA differs in about 13% and the cut-off wavelength obtained experimentally is remarkably larger than the nominal value. We investigated the origin of this apparent disagreement in the cut-off wavelength. We performed an auxiliary experiment to investigate the cutoff wavelength of the fiber using the conventional method [15]. We used an halogen lamp and an OSA to measure the transmission spectrum. This experiment was done with sections of fiber of 1 m in length. We found that the LP_{11} mode was guided up to 1.4 μm when the fiber was held straight. However, we observed that a small fiber curvature shifted the cutoff wavelength down to the nominal value, which indicates that the nominal value provided by the manufacturer is a practical parameter, but not the strict cutoff wavelength.

3.2 Group index and chromatic dispersion difference

The group index difference, Δn_g, and the chromatic dispersion difference, ΔD, between the LP_{01} and LP_{1m} modes were obtained from the modal effective index difference, Δn, using Eq. (2). The 1st and 2nd derivatives of Δn with respect to λ were found by fitting a proper function to the experimental measuremets of Δn, that was subsequently derived (the experimental data were fitted to polynomial functions by segments). The results corresponding to LP_{01}-LP_{11} for the two fibers are shown in Fig. 4. For both fibers, there is a wavelength range far below cutoff, where Δn_g is negative, meaning that the group index of the LP_{11} mode is larger than that of the LP_{01}. On the other hand, the dispersion rises as the wavelength approaches the cutoff of the LP_{11} mode. Theoretical calculations of Δn_g and ΔD for a 125 μm diameter step-index fiber with the fiber parameters that resulted from the best-fit of Δn (see Table 1) are also included. In general terms, the agreement between experimental and modelling results is rather good. However, there is a remarkable disagreement in the chromatic dispersion difference near the strict cutoff wavelength, where the theory predicts a sharper peak. We believe that the origin of such disagreement lies in the model that has been assumed for the fiber that involves a perfect step-index profile.

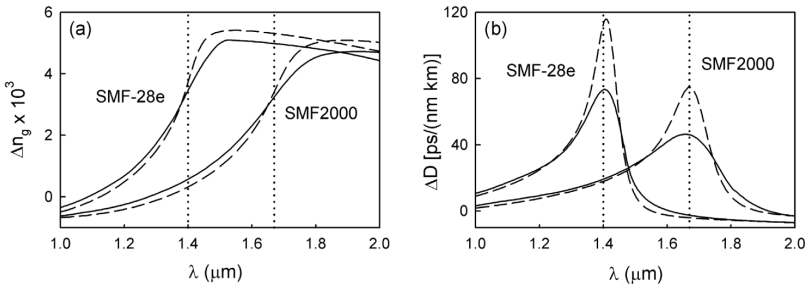

Fig. 4. (a) LP01-LP_{11} group index difference and (b) chromatic dispersion difference vs. wavelength. Solid lines are obtained from experimental measurements. Dashed line are theoretical calculations. Vertical dotted lines indicate the cut-off wavelength values obtained in section 4.1.

The group index difference between the LP_{01} and LP_{1m} modes with m = 2 - 5 is shown in Fig. 5 for the SMF-28e fiber. Within the wavelength range of our experimental arrangement, the LP_{1m} (m > 1) modes are cladding modes. It is known that the cut-off of a guided mode affects the guiding properties of higher order modes whose fields have the same angular order. Using the acousto-optic method, we were able to investigate the perturbation of the group index in LP_{1m} modes (with m > 1) as a result of the cut-off of the LP_{11} mode. Figure

#255185 Received 4 Dec 2015; revised 22 Jan 2016; accepted 27 Jan 2016; published 26 Feb 2016

5(a) shows the experimental result. For comparison, the corresponding theoretical calculation is shown in Fig. 5(b). Δn_g shows a bent at wavelengths near the LP_{11} cut-off wavelength, which is more clear for LP_{12} and LP_{13} modes.

3.3 Vector modes: TE, TM, and hybrid

The fine mode structure of LP_{1m} modes can also be investigated. It is known that the LP_{11} mode results from the superposition of three vector modes: TE_{01}, TM_{01}, and two HE_{21} modes with orthogonal polarizations. In conventional fibers, the triplet of modes are nearly degenerated, so they propagate with very similar phase velocity. As a result, when a LP_{11} mode is excited by the elastic wave, the three notches caused by the coupling from the fundamental HE_{11} mode are usually overlapped, giving rise to just one notch. However, the bandwidth of the notches depends on the length of the elastic grating: the longer is the elastic grating, the narrower are the notches. Therefore, the resolution of the characterization technique can be adjusted and the three notches can be observed separately provided that interaction length and uniformity of the fiber, are sufficient. So, we repeated the experiments with 50 cm of SM2000 fiber. Inset of Fig. 6(a) shows an example of the spectrum recorded when the elastic wave was adjusted to excite the LP_{11} mode. Now, three notches that result from the coupling to the triplet of modes modes are observed. Figure 6 shows Δn as a function of wavelength for the three modes. As expected, the splitting is larger as the wavelength approaches the cut-off wavelength. Far from cut-off, the modes are nearly degenerated. Even so, the AO technique can distinguish the three notches up to the point where the difference in modal effective index between the vector modes was as small as 3×10^{-6}.

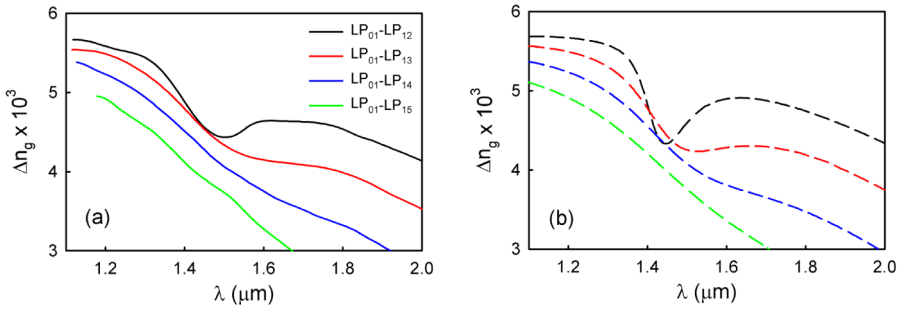

Fig. 5. LP01-LP_{1m} (m = 2 - 5) group index difference vs. wavelength. (a) Experimental result, and (b) theoretical calculations. FUT: SMF-28e.

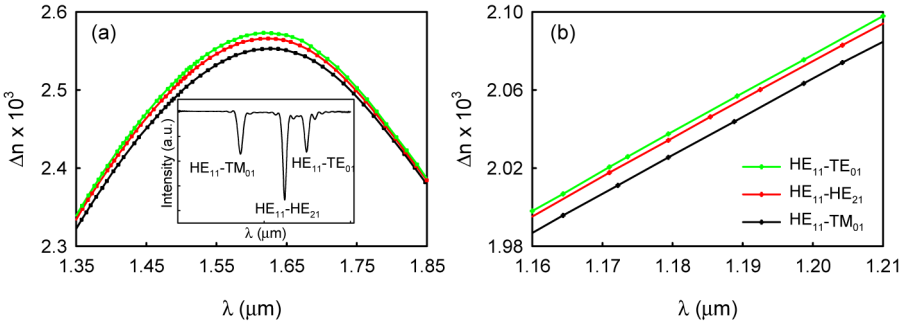

Fig. 6. Modal index difference vs. wavelength. (a) For wavelengths near cut-off and (b) for wavelengths well below cutoff. Inset shows a transmission spectrum. FUT: SM2000. Interaction length: 50 cm

#255185 Received 4 Dec 2015; revised 22 Jan 2016; accepted 27 Jan 2016; published 26 Feb 2016

4. Conclusions

Accurate mode characterization of two-mode optical fibers can be performed using in-fiber acousto-optic interaction. The effective index difference between modes was measured in a broad wavelength range around the LP_{11} cut-off wavelength. NA and λ_c were determined precisely and without ambiguity by fitting the experimental data to theoretical calculations based on a step-index model. Modal group index difference and modal chromatic dispersion difference were also obtained from the experiment, and were compared to theoretical calculations showing good agreement. Additionally, the fine mode structure of LP_{1m} modes, and other interesting features were also investigated by means of this technique.

Acknowledgments

Financial support from the Ministerio de Economía y Competitividad of Spain and FEDER funds (project TEC2013-46643-C2-1-R), and the Generalitat Valenciana (project PROMETEOII /2014/072) is acknowledged.

#255185 Received 4 Dec 2015; revised 22 Jan 2016; accepted 27 Jan 2016; published 26 Feb 2016